Electronic Supplementary Information (ESI)

Self-assembling tetrameric peptides allow *in situ* 3D bioprinting under physiological conditions

Sakandar Rauf,[a] Hepi H. Susapto,[a] Kowther Kahin, [a] Salwa Alshehri,[a] Sherin Abdelrahman,[a] Jordy Homing Lam, [b,c] Sultan Asad,[a] Sandip Jadhav,[a] Dhakshinamoorthy Sunderamoorthy[a] , Xin Gao[b,c] and Charlotte A. E. Hauser[a,b]*

[a]Laboratory for Nanomedicine, Division of Biological & Environmental Science & Engineering (BESE), and [b]Computational Bioscience Research Center (CBRC), [c]Computer, Electrical and Mathematical Sciences and Engineering (CEMSE) Division, King Abdullah University of Science and Technology (KAUST), Thuwal 23955-6900, Saudi Arabia.
E-mail: charlotte.hauser@kaust.edu.sa

Molecular Dynamics Simulation Videos:

Video 1. Simulation on Assembly of 4 IVFK peptides in a period of 100 ns.

Video 2. Simulation on Assembly of 4 IVZK peptides in a period of 100 ns.

Video 3. Simulation on Assembly of 60 IVFK peptides in a period of 100 ns.

Video 4. Simulation on Assembly of 60 IVZK peptides in a period of 100 ns.

3D Bioprinting Videos*:* Video 5-8 shows *in situ* 3D bioprinting of peptides into different shapes such as grids, text and 3D circles using the robotic arm 3D bioprinter.

Video 5: Shows 3D bioprinting of a ring structure in real time. The peptide IVZK (15mg) was dissolved in 1ml aqueous solution (0.006 % w/v) adding methylene blue dye to the peptide solution to make the printing process and the shape fidelity of the structure more easily visible. At the end of the bioprinting, MilliQ water was added to the printed ring structure. The video shows that the dye was incorporated inside the printed peptide hydrogel. The snapshot pictures shown here were taken from Video 5 right after the ring structure was printed, and while the robotic arm was moving upwards. These pictures and Video 5 clearly show that the peptide hydrogel was generated *in situ* during the printing process.

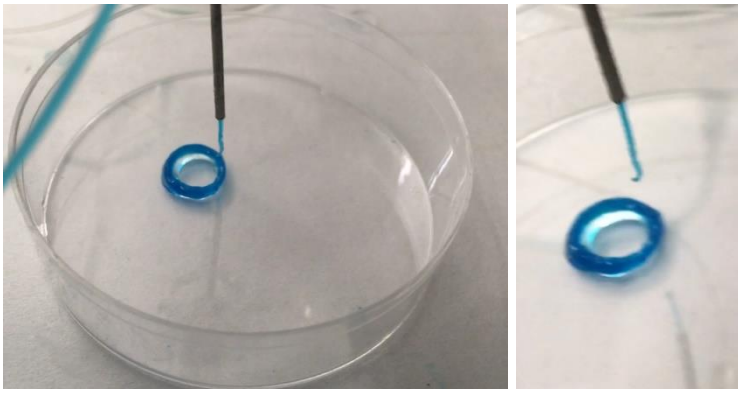

Video 6 (Time-lapse video): Shows the printing of a grid structure

Video 7 (Time-lapse video): Shows the printing of the text.

Video 8 (Time-lapse video): Shows the printing of 3D circular shape. The diameter of the circle is 10 mm and height is 20 mm.

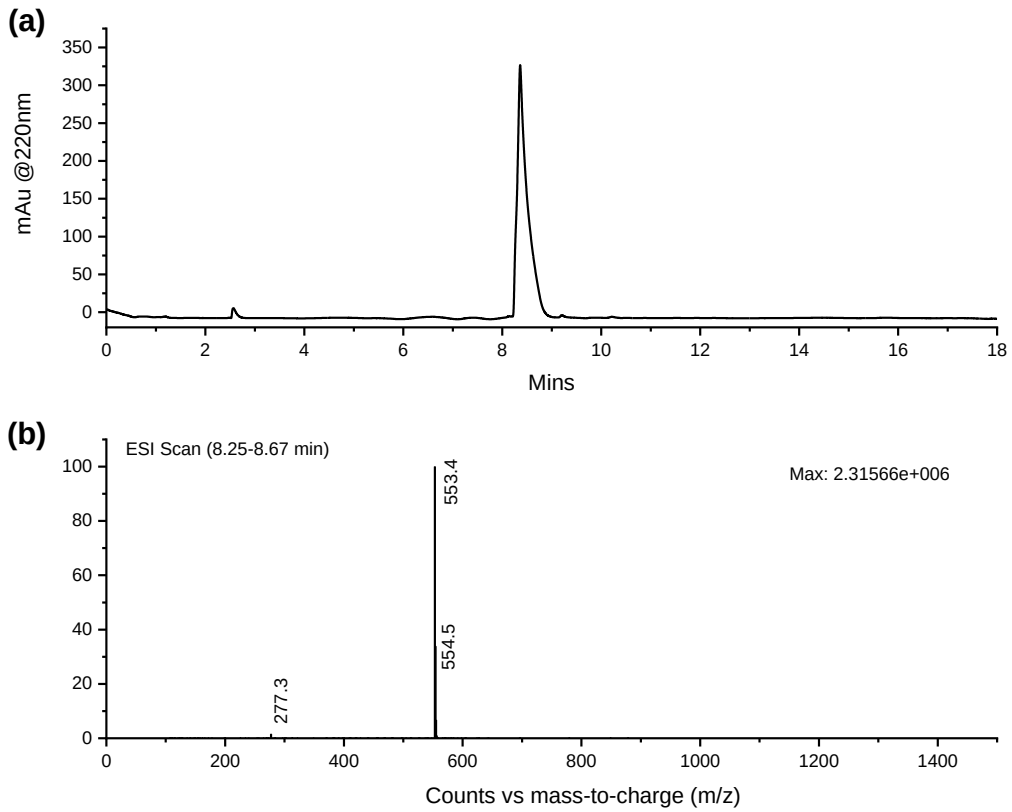

Fig. S1 Characterization of IVZK by using LC-MS. (a) Liquid chromatogram of IVFK by the absorbance at 220 nm. (b) Mass spectrum of IVFK. MS: (m/z) calculated 552.8, $[M+H]^+$ found 553.4, and $[M+2H]^{2+}$ found 277.3. The purity of IVZK peptide from chromatogram was found around 96.9%.

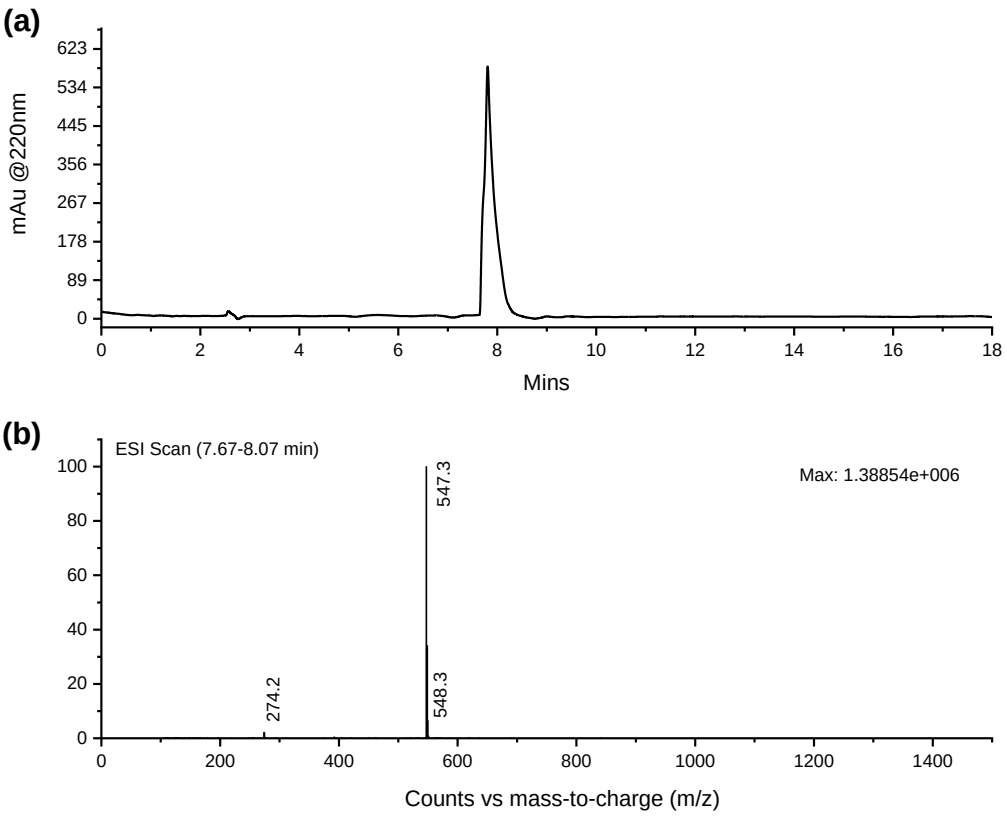

Fig. S2 Characterization of IVFK by using LC-MS. (a) Liquid chromatogram of IVFK by the absorbance at 220 nm, and (b) Mass spectrum of IVFK. MS: (m/z) calculated 546.7, $[M+H]^+$ found 547.3, and $[M+2H]^{2+}$ found 274.2. The purity of IVFK peptide from chromatogram was found around 99.2%.

^{1}H-NMR assignment for IVZK and IVFK

- IVZK Peptide:

^{1}H NMR (500 MHz, 9.03 mM in DMSO-d_6) δ 7.96 (d, *J* = 8.2 Hz, 1H), 7.94 (d, *J* = 6.8 Hz, 1H), 7.83 (d, *J* = 8.85 Hz, 1H), 7.80 (d, *J* = 8.15 Hz, 1H), 7.68 (bs, 3H), 7.26 (s, 1H), 7.05 (s, 1H), 4.30 (m, 1H), 4.19 - 4.11 (m, 3H), 2.74 (t, *J* = 7.7 Hz, 2H), 1.93 (m, 1H), 1.85 (s, 3H), 1.71 – 1.57 (m, 7H), 1.53 – 1.40 (m, 6H), 1.33 – 1.23 (m, 3H), 1.17 – 1.04 (m, 4H), 0.90 (m, 1H), 0.83 – 0.79 (m, 13H).

- IVFK Peptide:

^{1}H NMR (500 MHz, 9.15 mM in DMSO-d_6) δ 8.01 (d, *J* = 7.9 Hz, 1H), 7.98 (d, *J* = 8.2 Hz, 1H), 7.96 (d, *J* = 8.5 Hz, 1H), 7.72 (d, *J* = 8.9 Hz, 1H), 7. 70 (bs, 3H), 7.23 (d, *J* = 4.3 Hz, 4H), 7.17 (m, 1H), 7.11 (bs, 1H), 7.06 (bs, 1H), 4.55(m, 1H), 4.16 – 4.08 (m, 3H), 3.01 (m, 1H), 2.80 (m, 1H), 2.74 (m, 2H), 1.87(m, 2H), 1.85 (s, 3H), 1.66 (m, 1H), 1.50 (m, 3H), 1.40 (m, 1H), 1.28 (m, 2H), 1.05 (m, 1H), 0.80 - 0.72 (m, 12H).

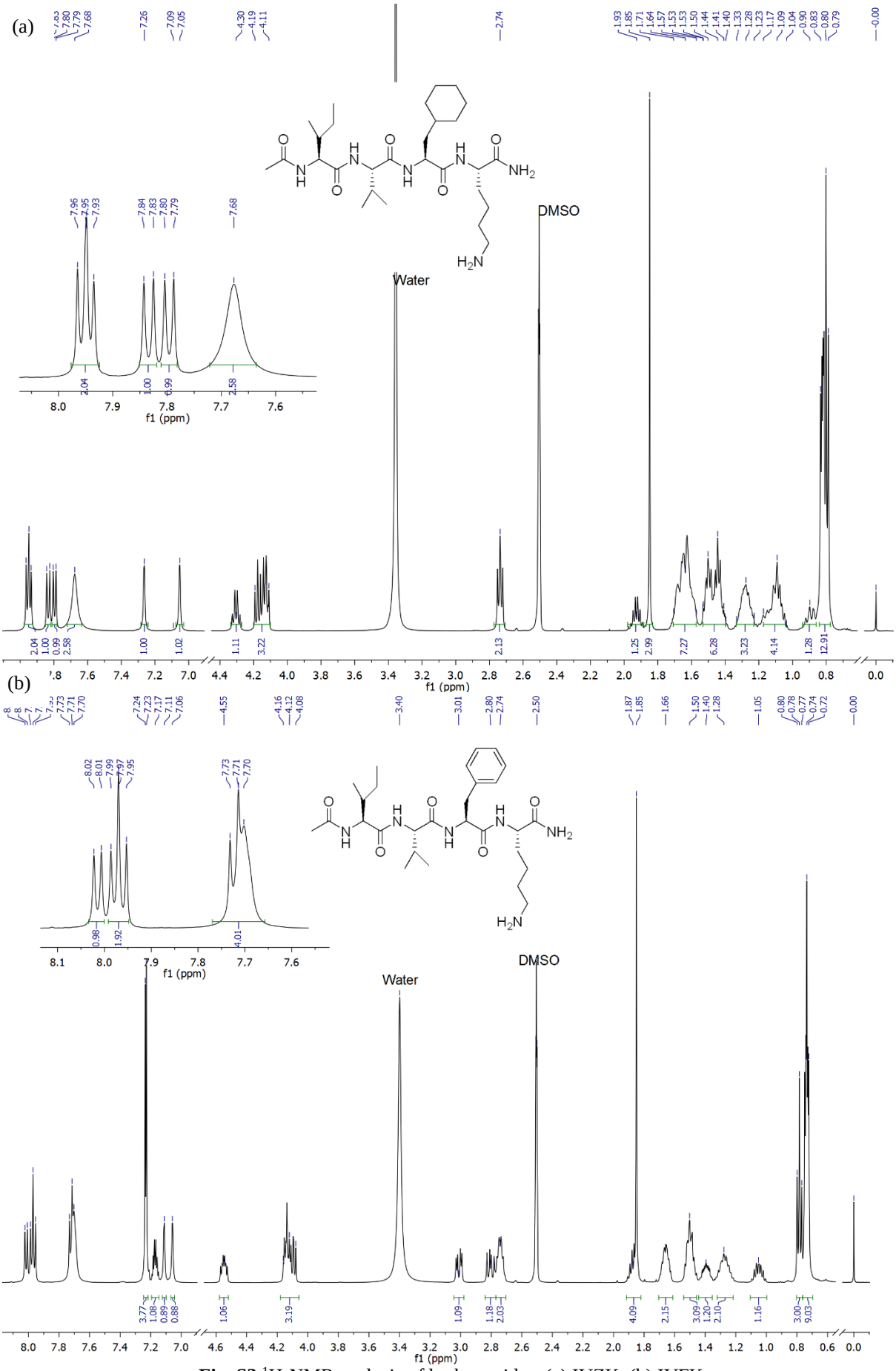

Fig. S3 ^{1}H-NMR analysis of both peptides. (a) IVZK. (b) IVFK

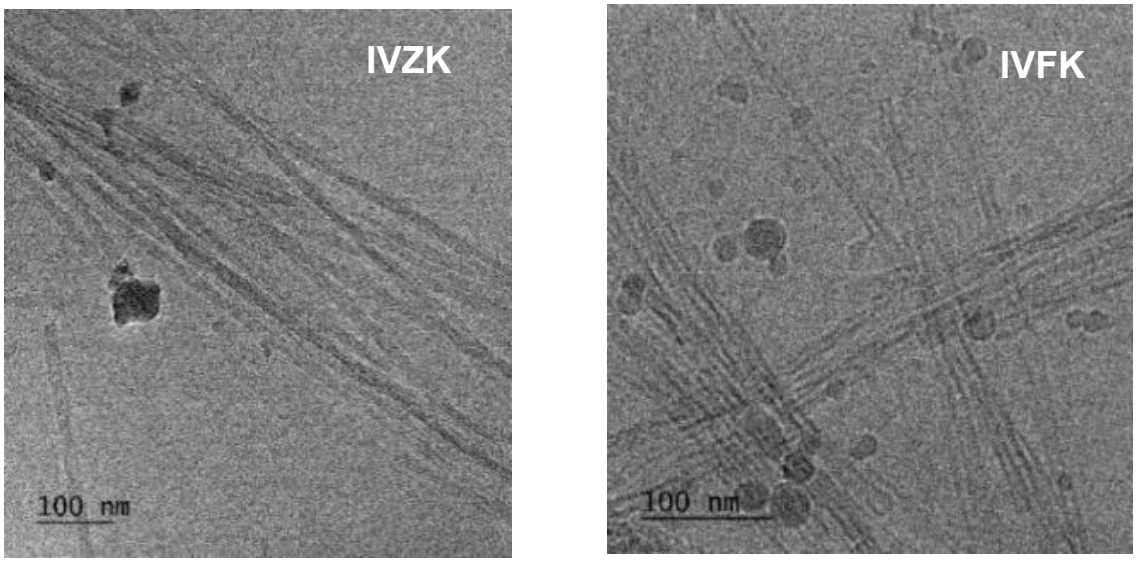

Fig. S4 The Cryo TEM images show two different morphologies in the case of IVZK and IVFK.

Conc.	IVFK				IVZK			
3 mg/ml	> 0 min	2 mins	5 mins	10 mins	> 0 min	2 mins	5 mins	10 mins
								
	20 mins	30mins	40 mins					
								
4 mg/ml	> 0 min	2 mins	5 mins	10 mins	> 0 min	2 mins	5 mins	10 mins
								
	20 mins							
								
5 mg/ml	> 0 min	2 mins	5 mins	10 mins	> 0 min	2 mins	5 mins	
								
8 mg/ml	> 0 min	2 mins			> 0 min			
								

Fig. S5 Characterization of gelation time of IVZK and IVFK peptides. (a) Different concentrations of both peptides were tested at different time intervals to form a hydrogel in the presence of PBS. > 0 min shows the results right after mixing the PBS with the peptide solution. In case of 8mg/ml instantaneous gelation was observed right after mixing the peptide solution and phpshate buffer.

Table S1

	Ac-IVZK- NH_2	Ac-IVFK-NH_2
Box Size	4.8	4.8
Number of Water	3933	3935
Number of Peptides	4	4
Net Charge in peptide	0	0
Mole Fraction	0.001	0.001
Speed on Shaheen	51ns/1day/192cores	51ns/1day/192cores

Table S2

	Ac-IVZK- NH_2	Ac-IVFK- NH_2
Box Size	7.8	7.0
Number of Water	13639	9470
Number of Peptides	60	60
Net Charge in peptide	0	0
Mole Fraction	0.004	0.006
Speed on Shaheen	45ns/1day/512cores	50ns/1day/512cores

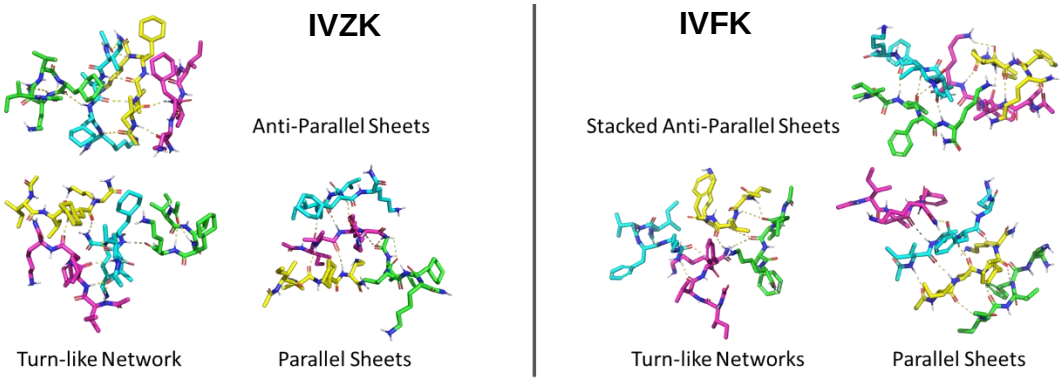

Fig. S6 Multiple conformers formed during the four IVZK and IVFK peptides assembly.

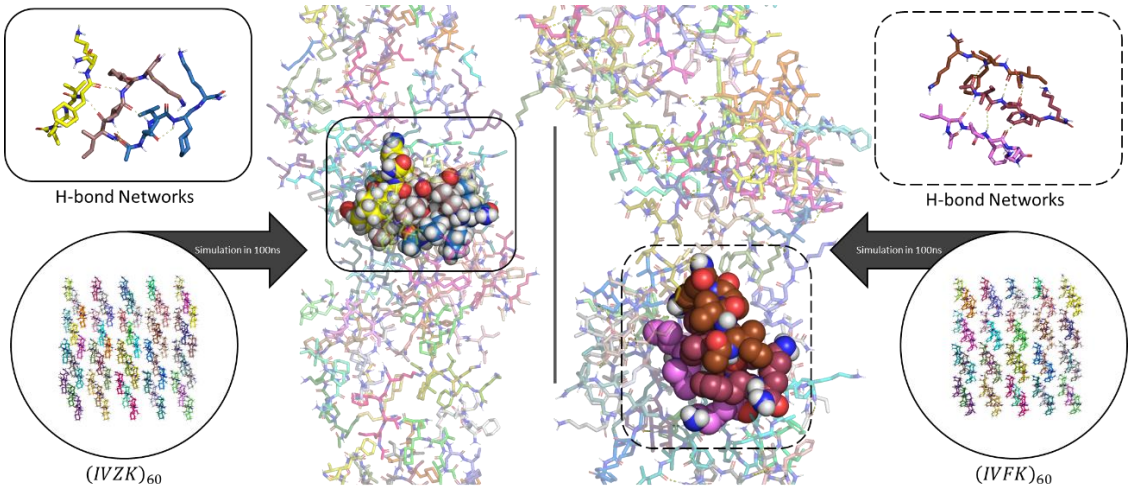

Fig. S7 Sheet structures as observed in fibers of 60-peptide Assembly. Parts in space-filled representation is zoomed as a licorice representation shown on the top right (IVZK) /left (IVFK) corner.

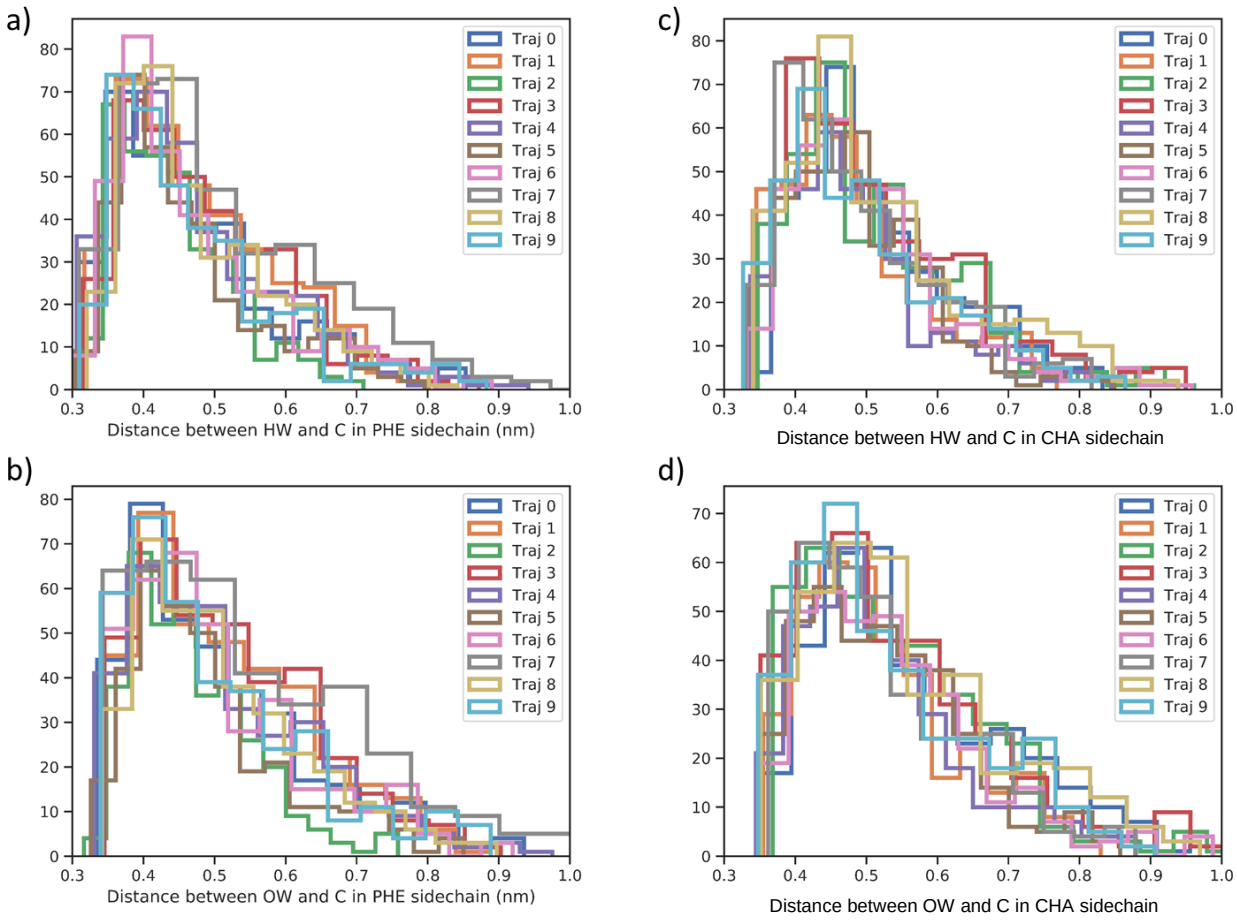

Fig. S8 Z is less solvent accessible than F. Distribution of distance between closest water (hydrogen atom HW and oxygen atom OW) and sidechain carbons in F (PHE, a and b) and Z (CHA, c and d).

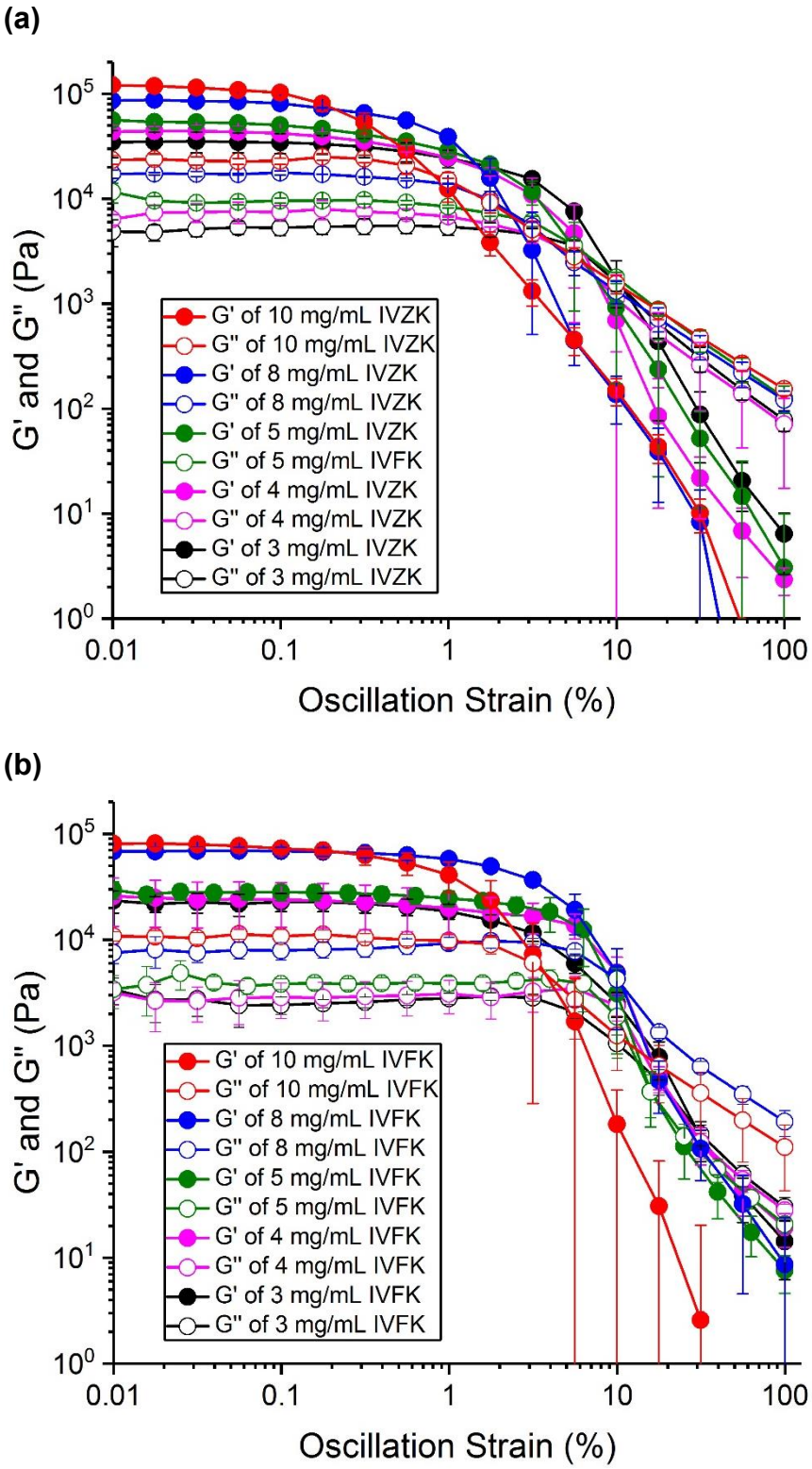

Fig. S9 Rheological characterization of IVZK and IVFK peptides. (a and b) shows the amplitude sweep (storage modulus G′ and loss modulus G″ as a function of strain γ) studies at different concentrations of IVZK and IVFK peptides.

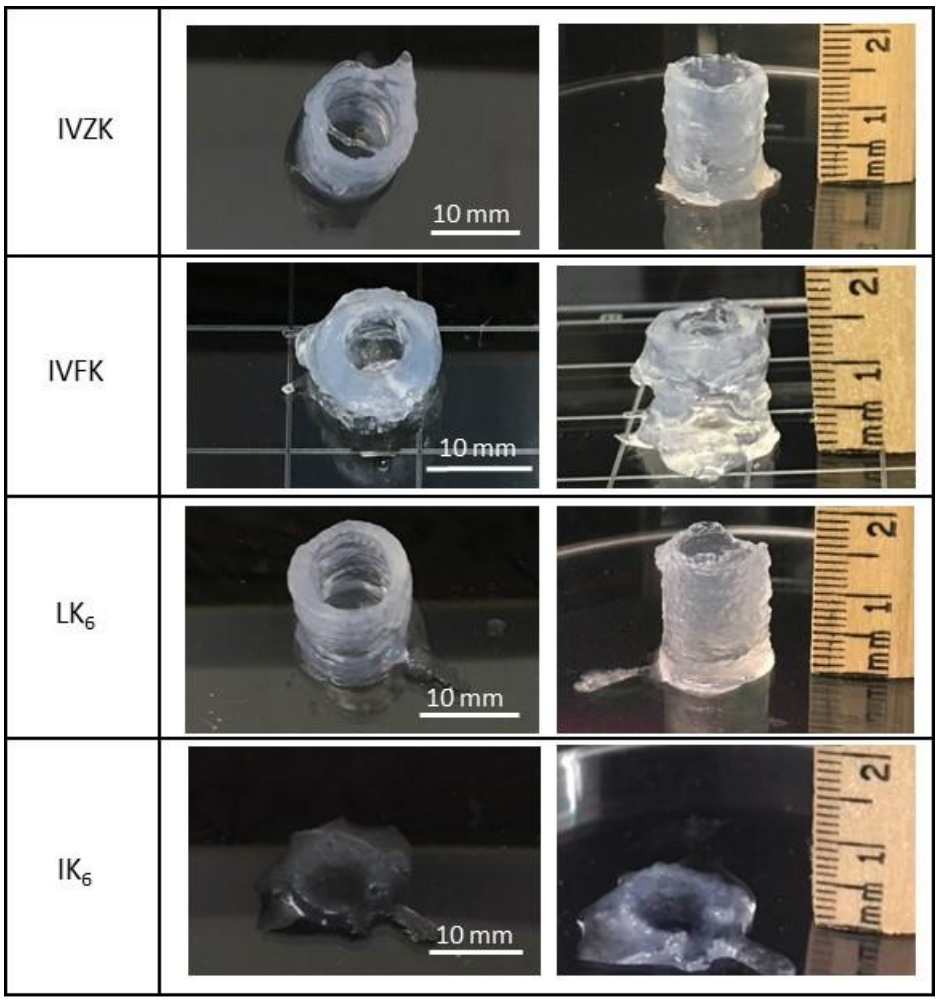

Fig. S10 Shows the printability of different peptides into hollow cylinder structures of diameter 10 mm and height of 15 mm. By comparing the printed structures of the peptides, IVZK was found to be the best performer among all other peptides in terms of ease in printing and long-term stability. LK_6 was better as compared to IVFK, and IK_6. Depending upon the peptide, different concentrations of peptides were used and tested (data not shown) to get the optimized peptide hydrogel from the nozzle. For IVZK, IVFK, LK_6 and IK_6 15 mg/ml, 15 mg/ml, 30 mg/ml and 10 mg/ml were used, respectively. The optimized flow rates for IVZK, IVFK, LK_6 and IK_6 were 55 µl/min, 55 µl/min, 45 µl/min and 50 µl/min, respectively. For IVFK and IK_6 peptides, flow rates were changed during the printing (± 5 µl/min) to obtain consistent hydrogel and well-defined structures. The flow rates of phosphate buffer (25 µl/min) and water (5 µl/min) were kept constant during all the printing experiments.

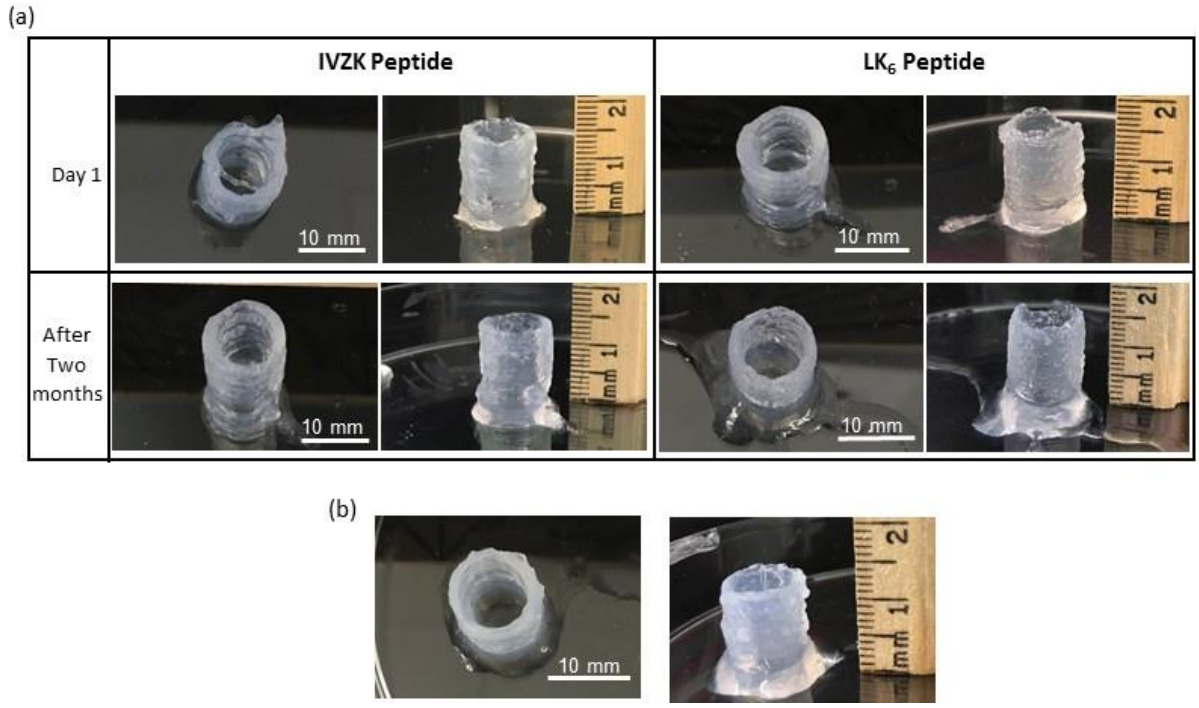

Fig. S11 (a) Comparison between two different peptides (IVZK and LK_6) showing the long-term stability and shape fidelity of the bioprinted structures at room temperature in a sealed petri dish from day 1 to after two months of printing and (b) demonstrates the stability of 3D bioprinted structures using IVZK peptide as bioink after three months storage at room temperature in a sealed Petri dish.

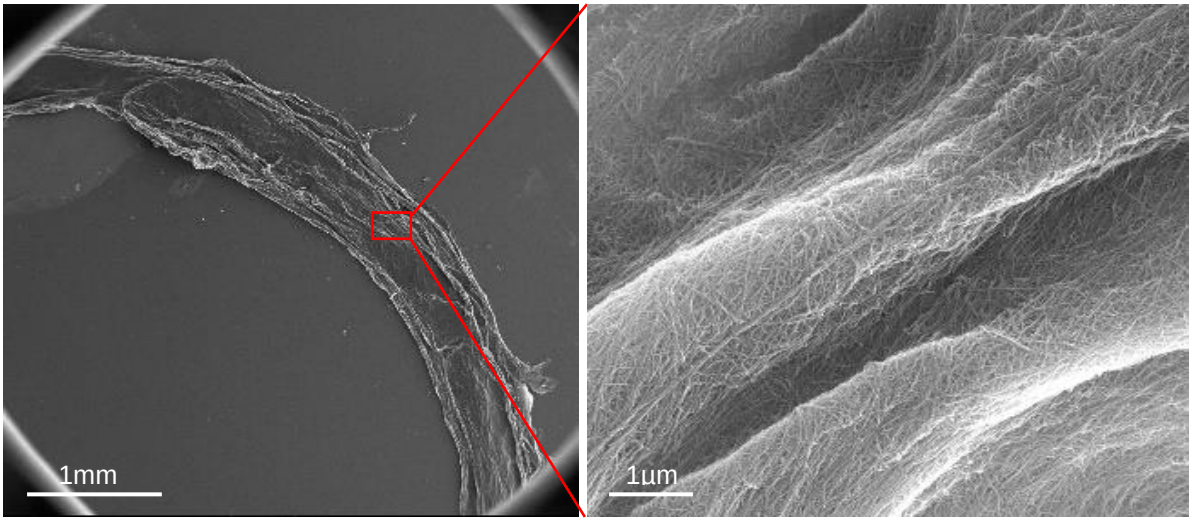

Fig. S12 Scanning electron microscopy (SEM) images of the 3D bioprinted IVZK peptide (15mg/ml) bioink. The SEM sample was prepared using critical point drying method as explained in the experimental section. Five peptide layers were bioprinted in this case.

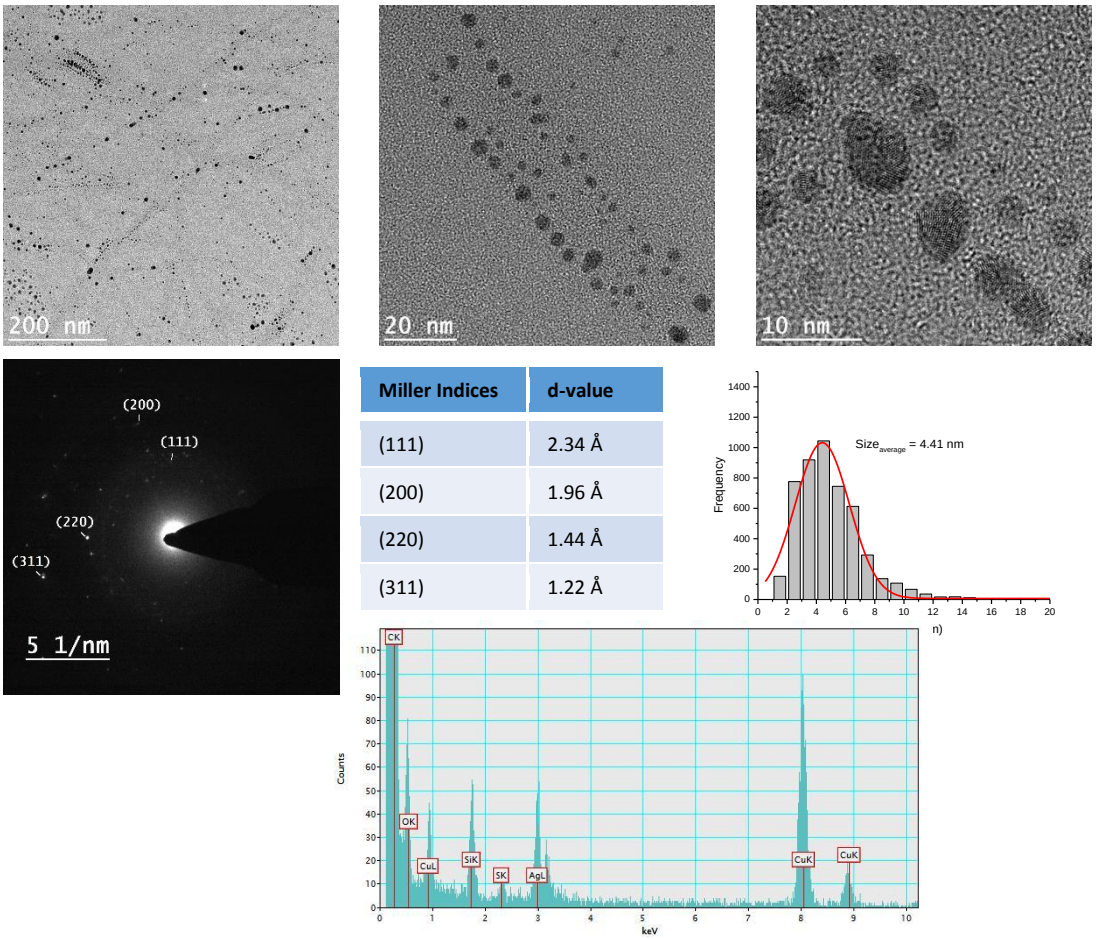

Fig. S13 Transmission electron microscopy studies of *in situ* generated silver nanoparticles using the 3D bioprinting method. The upper panel shows TEM images of silver nanoparticles at different magnifications. The lower panel shows the calculation of d-spacing for silver nanoparticles along with the EDX spectra confirming the presence of silver, and shows the size distribution curve of the silver nanoparticles (average diameter is 4.4 nm).

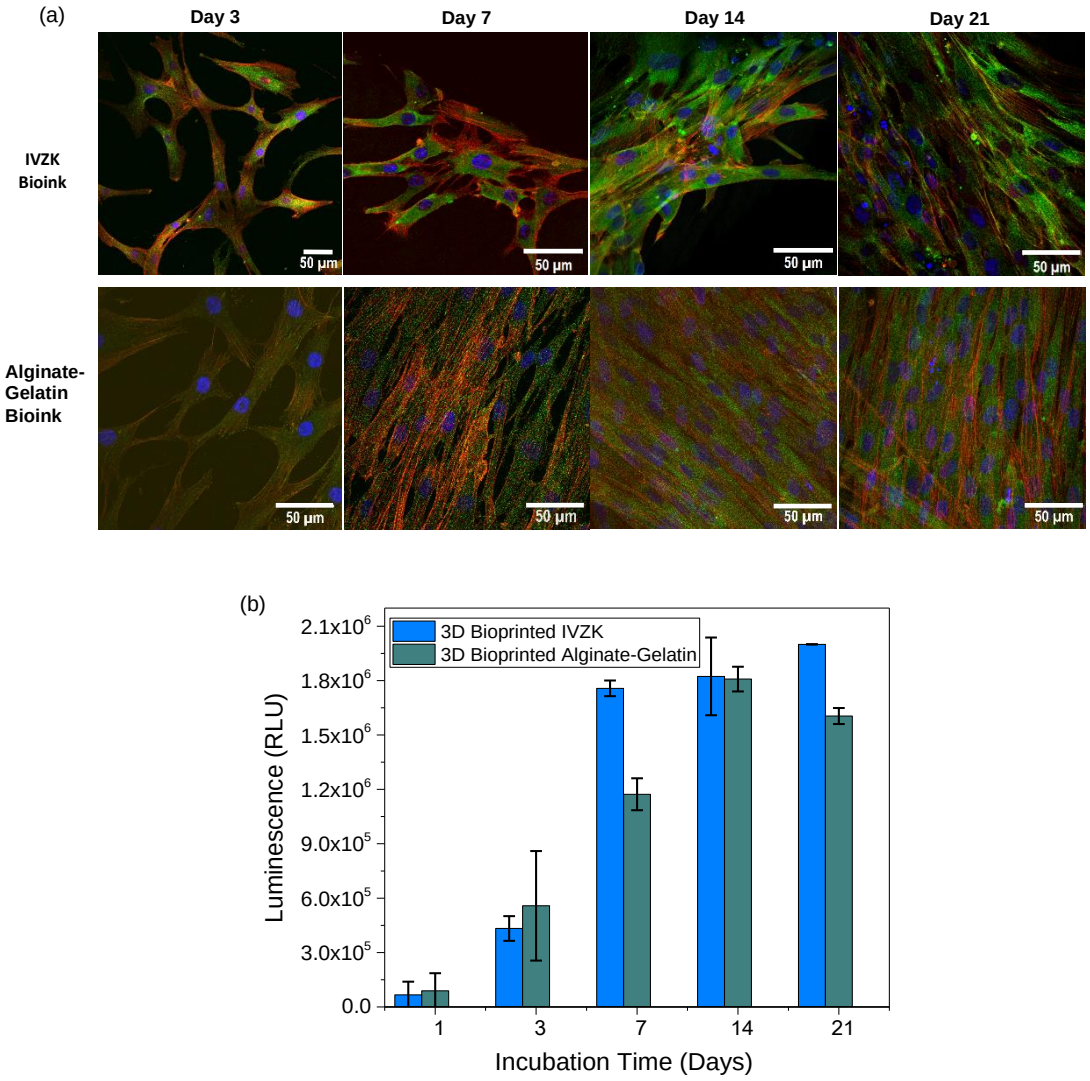

Fig. S14 Fluorescence confocal microscopy analysis of human bone marrow-derived mesenchymal stem cells (hBMSCs) 3D bioprinted using IVZK and alginate-gelatin bioinks. (a) Fluorescence confocal microscopy images of 3D bioprinted (BM-MSCs) cells using IVZK and alginate-gelatin bioinks at different days of cell culture (nucleus shown in blue, F-actin shown in red and vinculin in green). (b) 3D cell viability assay of BM-MSCs cells 3D bioprinted in IVZK and alginate-gelatin bioinks at various time points.

Author Contributions

C.A.E.H. conceived the idea of the project and together with S.R. designed the experiments with input from X.G., H.H.S. did the rheology, SEM, TEM and the NMR experiments. The 3D bioprinting experiments were done by S.R. and K.K., S. A., Sh. A., and D. S. did all cellular work, cell proliferation assays and confocal microscopy. S. R. was responsible for the work on silver nanoparticles and quantum dots. RNA sequencing was done by Sh. A. and sequencing analysis was done by S.A. MD simulation studies were done by J.H.L. and supervised by X.G. S.J. was taking care for the peptide synthesis. The manuscript was written through contributions of all authors. All authors have given approval to the final version of the manuscript.